A Hardware-in-the-loop Simulation Study of a Mechatronic System for Anterior Cruciate Ligament Injuries Rehabilitation

Juan C. Yepes[1,2], A. J. Saldarriaga[1], Jorge M. Vélez [1], Vera Z. Pérez[1,3] and Manuel J. Betancur[2,3]
[1]*Grupo de Investigaciones en Bioingeniería, Universidad Pontificia Bolivariana, Cir. 1 #73-76, B22C, Medellín, Colombia*
[2]*Grupo de Automática y Diseño A+D, Universidad Pontificia Bolivariana, Cir. 1 #73-76, B22C, Medellín, Colombia*
[3]*Facultad de Ingeniería Eléctrica y Electrónica, Universidad Pontificia Bolivariana, Cir. 1 #73-76, B22C, Medellín, Colombia*

Keywords: Rehabilitation Technology, Anterior Cruciate Ligament Injuries, Biorobotics, Motion Control, Exoskeleton, Goniometers, Hardware-In-the-Loop Simulation, Computed Torque Control Algorithm, Real-time Systems.

Abstract: One of the main ligaments of the knee is the Anterior Cruciate Ligament (ACL), which is critical to maintain stability and regular gait patterns. Moreover, the knee is the most complex and largest joint in the human body. There are many traditional methods and devices to assist therapy. Nevertheless, there are several research studies in robotic platforms for lower limb rehabilitation. This paper presents a hardware-in-the-loop (HIL) simulation of a movement control algorithm for mechatronic-assisted rehabilitation based on exercises and movements associated with therapies for ACL injuries. The implementation of the algorithm was conducted using a computational model in order to test the mechatronic system Nukawa without having to use the actual robot. Several tests were performed in order to validate the mathematical model of Nukawa. In order to assess whether the implemented HIL simulator works properly for ACL rehabilitation exercises, a physiotherapist performed six exercises and the movements were recorded with a commercial acquisition device, these trajectories were conducted to the HIL simulator. The Integral-Square-Error (ISE) was computed for each test, and since it was small, it may be despised. Therefore, the motion control algorithm is able to manipulate the three joints at the same time, hence it is possible to follow specific trajectories. In addition, the mean execution time $M = 11.5\ ms$ and the standard deviation $SD = 3.9$ taken by the controller is smaller than the sampling period, therefore we proposed that this system can be tested in real-time, without notable delays related to the movement control algorithm.

1 INTRODUCTION

In the European Union, almost 45 million people aged between 15 and 64 years had a disability during 2014, which corresponds to 14.1 % of that age group (Eurostat, 2014). According to the World Health Organization (WHO) in the last report, there are one thousand million people worldwide with some type of disability and about 200 million have function disabilities. Therefore, these people tend to have lower health and academic outcomes, lower economic participation and higher poverty rates than people without disabilities (World Health Organization, 2011). Nowadays people with some type of disability or difficult moving their lower extremities are people who have restrictions to participate in society, which affects interactions and relationships during civic, social and domestic life situations (Departamento Administrativo Nacional de Estadísctica, 2004).

The knee is the most complex and largest joint in the human body and it depends on four primary ligaments, tendons, muscles and secondary ligaments to maintain its correct functionality. One of the main ligaments is the Anterior Cruciate Ligament (ACL) (American Academy of Orthopaedic Surgeons, 2011). Due to great number of incidents, causing the premature end of high performance athletes careers caused by ACL injuries, monitoring process and rehabilitation protocols are applied. ACL is a critical ligament to maintain knee joint stability and regular gait patterns (Arosha Senanayake et al., 2014).

ACL is one of the most commonly injured ligaments in the knee, 150,000 ACL injuries occur each year in the United States of America and are estimated to cost half-billion dollars each year due to health care (American Academy of Orthopaedic Surgeons, 2011). Approximately 100,000 ACL reconstructions are applied in this country every year. In Hong Kong,

Yepes J., Saldarriaga A., VÃĺlez J., PÃŕrez V. and Betancur M.
A Hardware-in-the-loop Simulation Study of a Mechatronic System for Anterior Cruciate Ligament Injuries Rehabilitation.
DOI: 10.5220/0006252800690080
In *Proceedings of the 10th International Joint Conference on Biomedical Engineering Systems and Technologies (BIOSTEC 2017)*, pages 69-80
ISBN: 978-989-758-216-5

ACL injuries occur mostly during sports (in 89.3% of cases), being males with age between 18 and 30 years the most affected (Li and Ng, 2004). Nevertheless, women experience ACL tears nine times more often than men, studies have shown a 1.4 to 9.5 times increased risk of ACL tear in women (Cimino et al., 2010).

A direct blow to the knee is one of the ways to injure the ACL during sports or road traffic accident (Machhindra et al., 2016). Nevertheless, ACL injuries happen even without any contact with another object. These non-contact injuries occur mostly during changes of direction by the athlete while running or when landing from a jump if they hyperextend their knee (Cimino et al., 2010). A 4-year-study presented by Morey et. al. (Machhindra et al., 2016) reported that ACL injuries occur during sports (50%), a road traffic accident (46%), and other type of accidents (4%).

ACL does not heal itself and the standard method of treatment in young athletes is surgery but it is optional. The chance of rupturing the new ACL graft is of 5 %. After the surgery, a rehabilitation process is developed with the purpose of enabling the athletes to return to sports (Ganley, 2011). Recovering mobility, strength, quality of life and productivity of these subjects widely depends on physical rehabilitation therapies, achieving to return to sports and their daily activities.

There are many traditional methods and devices to assist therapy. Nevertheless, the study of new technologies applied in areas such as Bioengineering and Automation, has brought research and experimentation in robotic platforms that enables to replace, enhance or rehabilitate lower limb disabilities. Within these applications, robotic systems have become in a benefit for the rehabilitation in lower limb pathologies (Dollar and Herr, 2008). These studies have been focused on the development of powered lower-limb orthoses and exoskeletons (Guizzo and Goldstein, 2005) (Akdogan and Adli, 2011) (Yan et al., 2015). An exoskeleton is a biomechanic system coupled to the outside of the human body and offers an intelligent processing system to sense and to make decisions during the execution of functions through the actuators to reproduce the movement of the lower limb of a person (Blaya and Herr, 2004) (Eby, 2005). The main characteristic of these human-machine interfaces is that the contact between the user and the exoskeleton allows to transfer mechanical power and information signals (Pratt et al., 2004).

In order to control the movement of the joints of a mechatronic system, a control algorithm must be developed. It could be a classic or a modern algorithm; some examples of them are proportional-integral-derivative (PID) controller (Pan et al., 2015), Neuro-Fuzzy Control (Kiguchi et al., 2004), Computed Torque Control (CTC) (Lasso et al., 2010), among others. Also, there are many control schemes that can be used in order to control robotic exoskeletons such as impedance control, admitance control, force/torque control, position control, hybrid control (force/position). These control schemes depend on the specific application of the robotic system (Olaya, 2008). CTC is a model-based control. It enables compliant robot control with small tracking errors for precise robot models. The controller moves the robot, which is governed by the system dynamics. The tracking control determines the joints torque such that the robot follows the desired trajectory q_d, velocities $\dot{q}_d$ and accelerations $\ddot{q}_d$ of the robot (Nguyen-Tuong and Peters, 2008).

This paper presents a simulation of a movement control algorithm for mechatronic-assisted rehabilitation based on exercises and movements associated with therapies for ACL injuries. The implementation of the CTC algorithm was conducted as a hardware-in-the-loop (HIL) simulation using a computational model in order to test the mechatronic system Nukawa without having to use the actual robot.

This paper is presented as follows. Section 2 explains the methodology of the research, *i.e.*, the mathematical modeling of the mechatronic system Nukawa, and a wide description of each of the tests that were conducted in order to test and asses the movement control algorithm implemented as a HIL simulation and the model itself. In the first test, the mathematical model was conducted to several tests in order to validate it. Within the second test, the movement algorithm followed the actual movements conducted by a physiotherapist during several exercises that belong to international protocols for rehabilitation of ACL injuries. Section 3 shows results of the application of the methodology. Subsequently, we present the discussion in section 4. Finally, section 5 presents the conclusions regarding the results and possible future works.

2 METHODOLOGY

We are currently developing a system called "Nukawa", which is a mechatronic system for lower limb rehabilitation, and it has its antecedents in the LegSys system (Patiño et al., 2013) (Kirby, 2016). Figure 1 presents the CAD model of the Nukawa system. The mechatronic system Nukawa is product of the requirements presented by an interdisciplinary

group formed by physiotherapists, industrial designers and engineers. The design consists of two limbs, each one composed by a three-link mechanism and an electronic position control. The design also has brushless motors, power drivers, position and micro deformation sensors.

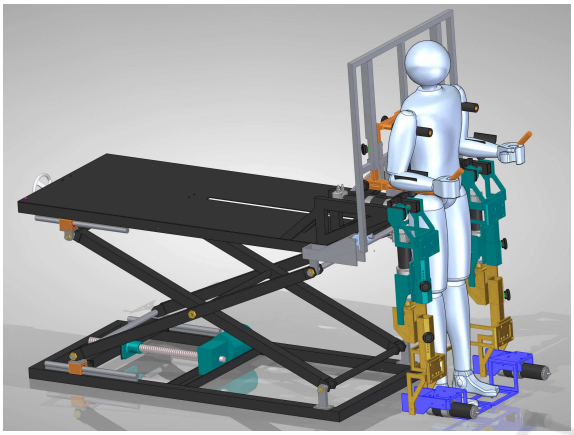

Figure 1: Nukawa, the mechatronic rehabilitation device for lower limb rehabilitation.

The three degrees of freedom (DOF) allows the system to perform flexion/extension (FE) movements of the hip, FE movements of the knee, and dorsi/plantar flexion (DP) movements of the ankle (Patiño et al., 2013). In addition, the joints are collinear to human joints. The knee is a polycentric joint, however this simplification was conducted as presented by Zoss et. al. (Zoss et al., 2006) who involves a pure rotational joint in the sagittal plane. In order to adjust the system for each person, the length of each segment of the mechatronic system Nukawa is variable, *i.e.*, the length between each joint can be adjusted. The system is designed for people between 1.44 m and 1.85 m tall, using a telescopic mechanical system. Therefore, the hip/knee can be adjusted.In addition, the system was designed for people of no more than 85 kg weight.

The system dynamics was mathematically modeled using the Newton-Euler method (K. S. Fu, 1987). The mathematical model of Nukawa includes the weight and dimensions of both the mechatronic device and a subject between the ranges previously stated. For this task, the base of the robot was supposed as fixed to the platform and the element 0 is stationary, therefore the initial conditions were assumed as angular speed $\omega = \dot{\omega}_0 = 0$, the linear speed $v_0 = 0$, the center of mass was assumed in the distal point of each limb, *i.e.*, being this the worst case, and therefore obtaining torques greater than the real ones, and $\dot{v_0}$ is

$$\dot{v_0} = \begin{pmatrix} g_x \\ g_y \\ g_z \end{pmatrix} \quad (1)$$

The model was implemented in the computational programming environment Matlab, and right after that a simplified and graphical model, which includes the robotic system and the subject, was implemented in order to test and assess the performance of the movement of the mechatronic device (Patiño et al., 2013) (Kirby, 2016). Table 1 presents the parameters of the physical model of the robotic system Nukawa, including the parameters of a subject of 1.85 m height and 83 kg weight.

Table 1: Nukawa, physical model parameters including a subject of 1.85 m height and 83 kg weight.

Variable	Description	Value	Unit
kfr1	Friction in hip joint	40	-
kfr2	Friction in knee joint	40	-
kfr3	Friction in ankle joint	40	-
L1	Link 1 length	0.4607	m
L2	Link 2 length	0.4755	m
L3	Link 3 length	0.3278	m
m1p	Thigh weight	12.2674	kg
m2p	Shank weight	3.9923	kg
m3p	Foot weight	1.1371	kg
m1e	L1 weight	19	kg
m2e	L2 weight	9	kg
m3e	L3 weight	11	kg
g	Gravity	9.8	$\frac{m}{s^2}$
Kp	Proportional Constant	150	-
Td	Derivative Time	0.1	-
m1Saturation	Motor 1 saturation	768.458	Nm
m2Saturation	Motor 2 saturation	371.377	Nm
m3Saturation	Motor 3 saturation	102.689	Nm

Taking into account that $m1 = m1p + m1e$, $m2 = m2p + m2e$, and $m3 = m3p + m3e$. Also, $q1$, $q2$, and $q3$ are the angles of the hip, knee and ankle joint, respectively. The mass matrix was represented by $M(q)$, the centripetal and coriolis effects were represented by $V(q,\dot{q})$, and the gravitational effects are represented by $G(q)$.

$$M(q) = \begin{pmatrix} M_{1,1} & M_{1,2} & M_{1,3} \\ M_{2,1} & M_{2,2} & M_{2,3} \\ M_{3,1} & M_{3,2} & M_{3,3} \end{pmatrix} \quad (2)$$

$$\begin{aligned} M_{1,1} = {} & m3 * L3 * (L1 * cos(q2+q3) + L2 * cos(q3) \\ & + L3) + m2 * L2 * (L1 * cos(q2) + L2) + m3 * L2 \\ & (L1 * cos(q2) + L2 + L3 * cos(q3)) + m1 * L1^2 \\ & + m2 * L1 * (L1 + L2 * cos(q2)) + m3 * L1 * (L1 \\ & + L2 * cos(q2) + L3 * cos(q2+q3)) \end{aligned} \quad (3)$$

$$M_{1,2} = m3*L3*(L2*cos(q3)+L3) + m2*L2^2 + m3*L2*(L2 + L3*cos(q3)) + m2*L1*L2*cos(q2) + m3*L1*(L2*cos(q2)+L3*cos(q2+q3)) \quad (4)$$

$$M_{1,3} = m3*L3^2 + m3*L2*L3*cos(q3) + m3*L1*L3*cos(q2+q3) \quad (5)$$

$$M_{2,1} = m3*L3*(L1*cos(q2+q3)+ L2*cos(q3)+L3) + m2*L2*(L1*cos(q2)+L2) + m3*L2*(L1*cos(q2)+L2+L3*cos(q3)) \quad (6)$$

$$M_{2,2} = m3*L3*(L2*cos(q3)+L3) + m2*L2^2 + m3*L2*(L2+L3*cos(q3)) \quad (7)$$

$$M_{2,3} = m3*L3^2 + m3*L2*L3*cos(q3) \quad (8)$$

$$M_{3,1} = m3*L3*(L1*cos(q2+q3) + L2*cos(q3)+L3) \quad (9)$$

$$M_{3,2} = m3*L3*(L2*cos(q3)+L3) \quad (10)$$

$$M_{3,3} = m3*L3^2 \quad (11)$$

$$V(q,\dot{q}) = \begin{pmatrix} V_{1,1} \\ V_{2,1} \\ V_{3,1} \end{pmatrix} \quad (12)$$

$$V_{1,1} = m3*L3*(L1*sin(q2 + q3)*q1p^2 + L2*sin(q3)*(q1p+q2p)^2) + m2*L1*L2*sin(q2)*q1p^2 + m3*L2*(L1*sin(q2)*q1p^2 - L3*sin(q3)*(q1p+q2p+q3p)^2) - m2*L1*L2*sin(q2)*(q1p+q2p)^2 - m3*L1*L2*sin(q2)*(q1p+q2p)^2 - L3*sin(q2+q3)*(q1p+q2p+q3p)^2 \quad (13)$$

$$V_{2,1} = m3*L3*(L1*sin(q2 + q3)*q1p^2 + L2*sin(q3)*(q1p+q2p)^2) + m2*L1*L2*sin(q2)*q1p^2 + m3*L2*(L1*sin(q2)*q1p^2 - L3*sin(q3)*(q1p+q2p+q3p)^2) \quad (14)$$

$$V_{3,1} = m3*L3*(L1*sin(q2 + q3)*q1p^2 + L2*sin(q3)*(q1p+q2p)^2) \quad (15)$$

$$G(q) = g*\begin{pmatrix} G_{1,1} \\ G_{2,1} \\ G_{3,1} \end{pmatrix} \quad (16)$$

$$G_{1,1} = m3*L3*cos(q1+q2+q3) + m2*L2*cos(q1+q2) + m3*L2*cos(q1+q2) + m1*L1*cos(q1) + m2*L1*cos(q1) + m3*L1*cos(q1) \quad (17)$$

$$G_{2,1} = m3*L3*cos(q1+q2+q3) + m2*L2*cos(q1+q2) + m3*L2*cos(q1+q2) \quad (18)$$

$$G_{3,1} = m3*L3*cos(q1+q2+q3) \quad (19)$$

The movement control algorithm was implemented using Python in a development platform. This process was conducted taking into account the mathematical model of the robotic system presented in Equations 2 - 19. The CTC algorithm was used in order to get gravitational compensation and to remove, or to depreciate, the nonlinearities of the system.

The algorithm was developed to work as a hardware-in-the-loop (HIL) simulation in order to test the algorithm without interacting with the actual robot, but enabling to extract data to assess the algorithm. The implementation was conducted in a development platform named Beaglebone Black (BBB) Rev C, which has AM335x 1GHz ARM® Cortex-8512MB processor and a 512 MB DDR3 Memory RAM. This implementation was conducted using Python, the high-level programming language. The BBB communicates with the mathematical model placed in a computer, through the TCP/IP protocol within a predefined communication port in order to allow remote execution. The sampling period was set to $TS = 0.02\ s$, therefore the sampling frequency was $f = 50\ Hz$. The computer used for the test had an Intel® Core™ i5 with a 4 GB DD3 memory RAM.

In order to control the movements of the Nukawa model, a desired trajectory for each joint must be established and then conducted to the CTC algorithm, *e.g.*, a knee flexion from 0 ° to 90 ° in 4 *s*. Each joint has a coordinate axis, and a counterclockwise movement is the convention for a positive arc of movement, and the angles are relative to the previous segment of the robot. The position $q = (0\,^\circ,\ 0\,^\circ,\ 0\,^\circ)$ means that the robot is fully extended, therefore the three joints should be at 0 °, however this position is not feasible for the human body. Therefore, the main positions of the mechatronic system Nukawa are presented in Figure 2. Figure 2(a) presents the supine position, *i.e.*, lying horizontally facing up by means of a $q = (0\,^\circ,\ 0\,^\circ,\ 90\,^\circ)$ position, and a backrest angle of 180 °. Figure 2(b) presents a sitting position by means of a $q = (0\,^\circ,\ -90\,^\circ,\ 90\,^\circ)$ position, and a backrest angle of 90 °. Finally, Figure 2(c) presents a standing position by means of a $q = (-90\,^\circ,\ 0\,^\circ,\ 90\,^\circ)$ position, , and a backrest angle of 90 °.

The CTC algorithm is responsible for computing the necessary torque in order to control the movement of each joint as desired. Thereby, the position of each limb and joint of the simplified model is modified as the desired path indicates it. The simulation of the dynamics of the system calculated within the computer in the Matlab is slow compared to TS. Nonetheless, the control algorithm was designed so that the time taken by simulation of the dynamics of the model will not affect the results of the movement, enabling to control the mechatronic device in Matlab.

2.1 Model Validation

In order to test and assess the dynamics, and the free motion of the mathematical model, we evaluated the behavior of the simulator without the controller, *i,e*, disabling the torque generated by the CTC, or just enabling some parts of it. Five different type of tests were conducted (A to E), and the mechatronic device was also initialized at several positions in order to perform several sub tests. In total eleven trials were conducted with the purpose of validating the model.

In order to compute the lengths and weights of the segments regarding a person from 1.44 *m* to 1.85 *m* height and from 50 *kg* to 100 *kg*, the models proposed by Plagenhoef (Plagenhoef et al., 1983) and De Leva (De Leva, 1996) were used. These models contain anatomical data for analyzing human motion. Table 2 presents the percentages of total body weight for each of segments of the lower limb. Table 3 presents the segment length as a percentage of total height. However, several models has been proposed in order to compute body measurements.

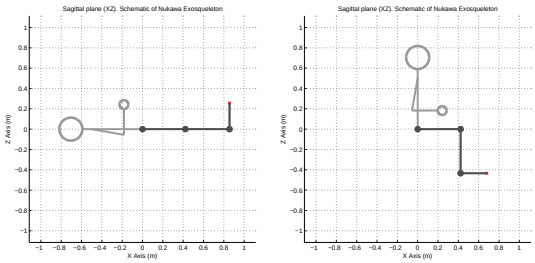

(a)

(b)

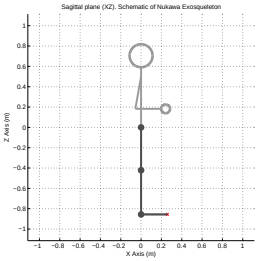

(c)

Figure 2: Main positions for the mechatronic system, (a) Supine position $q = (0\,^\circ, 0\,^\circ, 90\,^\circ)$, and a backrest angle of 180 °, (b) sitting position $q = (0\,^\circ, -90\,^\circ, 90\,^\circ)$, and a backrest angle of 90 °, and (c) standing position $q = (-90\,^\circ, 0\,^\circ, 90\,^\circ)$, and a backrest angle of 90 °.

Table 2: Percentages of total body weight (De Leva, 1996).

Segment	Males	Females	Average
Thigh	14.16	14.78	14.47
Shank	4.33	4.81	4.57
Foot	1.37	1.29	1.33

Table 3: Segment length as a percentage of total height (Plagenhoef et al., 1983).

Segment	Men	Women	Average
Thigh	23.2	24.9	24.05
Shank	24.7	25.7	25.2
Foot	4.25	4.25	4.25

2.2 Test with ACL Rehabilitation Exercises

In order to assess whether the implemented HIL simulator works properly for ACL rehabilitation exercises, several tests were conducted. With the assistance of a physiotherapist with a specialization on Biomedical Engineering a selection process of the exercises belonging to international protocols for rehabilitation of ACL injuries was performed.

Inclusion criteria were: (a) Exercises that can be performed with the rehabilitation system Nukawa (b) Exercises that only involve movements in the sagittal plane (c) Exercises involving only the movement of a leg (d) Exercises that are repeated at least in two

phases considering the Accelerated ACL Reconstruction Rehabilitation Program of Chester, the Classic 1981 Protocol, the Steadman Protocol, and (e) Assisted, resisted, and active exercises. Exclusion criteria were: (a) Isometric and isotonic exercises, and (b) Exercises involving trunk movement.

Subsequently, in order to validate that the robotic system Nukawa can follow the actual movements performed during the selected exercises, the physiotherapist performed each of the exercises, and the movements where recorded with a commercial acquisition device. During each exercise we ordered the expert to conduct the movements the best way possible, *i.e*, as it should be done so that the subject is rehabilitated.

Figure 3 presents the start/end point of the six exercises. Figure 3(a) and 3(g) presents the starting point and the ending point of an elevation of straight leg exercise, respectively. Figure 3(b) and 3(h) presents the starting point and the ending point of an unilateral leg press exercise, respectively. Figure 3(c) and 3(i) presents the starting point and the ending point of an assisted extension exercise, respectively. Figure 3(d) and 3(j) presents the starting point and the ending point of a progressive resisted quadriceps extension exercise, respectively. Figure 3(e) and 3(k) presents the starting point and the ending point of a progressive resisted hamstring flexion exercise, respectively. Figure 3(f) and 3(l) presents the starting point and the ending point of a Displacement of heel on bed exercise, respectively.

The acquisition device used to capture the movements performed by the expert in physiotherapy was the wearable body sensing platform BiosignalPlux powered by Plux®, the sampling rate was $fs = 1000\,Hz$. The sensed data was stored in a text file using the OpenSignals software, also powered by Plux®. The BiosignalPlux is a wireless device that enables to record and to sent real-time information captured by various sensors that can be connected. In order to capture the movements performed by the physiotherapist during the selected exercises, three twin axis goniometers (SG150) were used. However, the tests with the HIL simulation only used the flexion/extension channels of each goniometer in order to measure hip FE movements, knee FE movements, and ankle DP movements. The goniometers were located in the right leg, *i.e.*, the dominant lower limb member of the physiotherapist. Piriyaprasarth et. al. (Piriyaprasarth et al., 2008) reported the reliability of electrogoniometers and stated the importance of using a standard attachment protocol and standardized measurement procedures. Therefore, we followed some of the recommendations of the goniometer and torsiometer operating manual (Biometrics Ltd, 1998) from Biometrics Ltd ®.

The physiotherapist wore shorts to allow attachment of the goniometers. These sensors were located taking into account that they formed a "simple" bend, without forming an "Oxbow shape". The sensors were also located taking into account that the distance between the two endblocks of the goniometers were not reduced. Both cares were considered in order to not reduce the accuracy. The endblocks of the sensors were attached with a double-sided tape, and they were firmly pressed over the subject.

With the purpose of locating the ankle goniometer, the distal endblock was attached in the back of the heel of the physiotherapist, without the shoes. Subsequently, we asked the physiotherapist to execute the a dorsiflexion movement, until he reached his maximum range of motion (ROM). At this point, the proximal endblock was attached at the back of the leg, taking into account that both axes were coincident.

In order to locate the sensor on the knee joint, we asked the physiotherapist to stand, so that he was standing in the neutral position over a flat surface. The distal endblock was laterally located on the leg, so the axes of the leg and the endblock were coincident. Then, the goniometer was extended until it reached the maximum secure position recommended for the SG150 goniometers, this distance was measured with a vernier in order to ensure the distance between the to endblocks as suggested by the operating manual of the goniometers. Finally, with the goniometer extended, the proximal endblock was attached to the thigh, tanking into account that both axes were coincident.

In order to locate the sensor of the hip joint, we also asked the physiotherapist to stand on a flat surface. The proximal endblock was attached to the trunk, in the pelvic region. Subsequently, the goniometer was also extended until it reached its maximum recommended by the operating manual, this distance was also measured using a Vernier. The distal endblock was attached to the thigh, taking into account that the axis of the endblock and the axis of the thigh were coincident when observed in sagittal plane.

With all three goniometers attached to the joints of the physiotherapist (A), a calibration process was conducted with the help of another physiotherapist (B) and the BiosignalPlux. To do so, we asked the physiotherapist (A) to move each joint separately until he reached the maximum ROM of the joint. At this point, the physiotherapist (B) measured the angle with an analog goniometer, and we stored the exact value with a pushbutton in order to do a manual event annotation of the events. Both data were used to calibrate the angles of hip, knee, and ankle joints. The trajec-

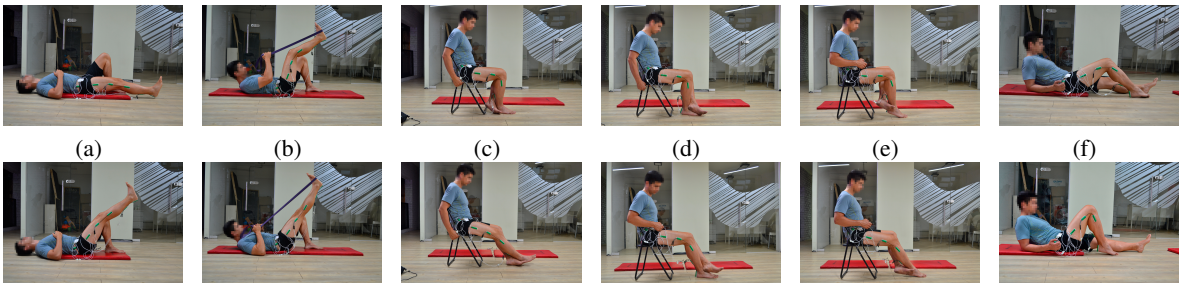

(a) (b) (c) (d) (e) (f)

(g) (h) (i) (j) (k) (l)

Figure 3: Start/end point of the six exercises.

tories or movements executed by the physiotherapist during the tests with the acquisition device, were filtered using a fifth-order Butterworth Low-pass filter with a cut-off frequency of $6\,Hz$ in order to soften the signal.

Subsequently, the pre-recorded angles of each joint were conducted to an offline simulator in order to validate the trajectories of the simulation that would be used with the HIL simulation. Figure 4 presents one of the six cases, which is the simulation of an elevation of straight leg exercise. This offline simulation was conducted using a 3D CAD model of Nukawa. This simulation included the kinematics of the robot.

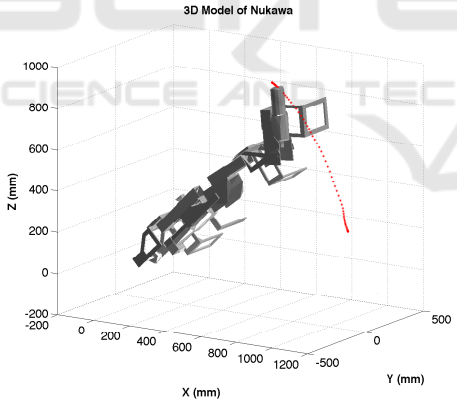

Figure 4: 3D Simulation with pre-recorded trajectories in order to validate the movements in the right limb of Nukawa.

Finally, the trajectories were conducted to the HIL simulation. These movements were a position reference, *i.e.*, the angles of the hip, knee, and ankle were conducted as a position references for the three joints of the robotic system. These movements associated with therapies for ACL injuries were also used in order to test and assess the movement control algorithm for mechatronic-assisted rehabilitation. The Integral Square Error (ISE) (Augusta, 2013) was calculated for each sub-test. In addition, we assessed whether each joint movements were within the range of motion (ROM) of the three joints of the lower limbs taking into account the values presented in Table 4. We also measured the execution time, *i.e.*, the time taken by the movement control algorithm in order to compute the torque of the three joints within each sampling period.

Table 4: Lower extremity range of motion (Nancy Berryman, 2002).

Joint	Movement	Range of Motion (°)
Hip	Flexion	122 ± 12
	Extension	22 ± 8
Knee	Flexion	134 ± 9
	Extension	-1 $\pm$ 2
Ankle	Dorsiflexion	12 ± 4
	Plantar flexion	54 ± 6

3 EXPERIMENTS AND RESULTS

In this section, we present the results of the experiments described in section 2. In the first group of experiments the mathematical model was conducted to several tests in order to validate it. The second group of experiments were carried out using six predefined position references regarding ACL rehabilitation exercises, in order to test the behavior of the movement control algorithm.

3.1 Results of the Model Validation

Table 5 presents the results of the eleven trials disabling some parts of the CTC algorithm. The response of the system, and a description is presented for each case. Each type of test is represented with a prefix letter; *i.e.* A, B, C, D, E; and the sub tests, using different initial positions of the rehabilitation system for the same test, are represented represented with a suffix number, *i.e.* A1, A2, A3. The input reference

was set to 'HOLD', by means of a static position. The difference between the desired and actual trajectories is evaluated through the ISE normalized and explanations about the behavior of the simulation are stated in the last column of table.

3.2 Results of the Test with ACL Rehabilitation Exercises

Table 6 presents the results of the six HIL simulation tests that we performed with predefined references, *i.e.*, using the trajectories acquired within the tests with the physiotherapists. This table shows the results of computing the ISE Normalized for each joint, these values represent the integration of the square of the error over time. It penalizes small errors, nonetheless it penalizes large error even more. Therefore, it is proposed that the CTC algorithm implemented within the BBB eliminates large errors quickly, but it tolerates small errors, which are needed for the PD controller to work.

Table 1 includes the values set to saturate the motors within the mathematical model. Table 6 shows that maximum torque exerted by controller for each joint, does not saturate the supposed motors. Therefore, the motors must meet this torque requirements, either by construction, or by means of gears, so that Nukawa may follow the proposed trajectories. Moreover, the motors must ensure the speed at those torques.

Table 6 also presents the maximum and minimum angle for each joint during all six tests. In this tables one can notice that the angles executed by the robotic system Nukawa are within the ROM of the lower limb of the human body. Therefore, the system is validated in the case that the CTC controller knows the exact parameters of the model. On the other hand, it is imperative to test the system using the entire range of lengths an weights available within the design.

Figure 5 contains six subfigures, each subfigure presents the result of HIL simulation for each of the exercise. The red and dotted line represents the actual endpoint of the robot, *i.e.*, the distal point of the third limb (L3). The blue dotted line represents the desired position trajectory for the endpoint of the robot. Consequently, it is proposed that the robotic system may conduct mechatronic-assisted rehabilitation based on exercises and movements associated with therapies for ACL injuries.

Figures 6, 7, and 8, present the results of the first exercise. Figure 6 compares the desired position in a continuous line, and the actual position with a dotted line. In this figure it is possible to observe that the system is able to follow the desired position reference, due to the fact that both are almost overlapped, with a delay. We can denote that the system correctly follows the imposed reference not only visualizing Figure 6 but for the error presented in Figure 7. Figure 8 presents the desired speed in continuous line and the actual speed in dotted line.

Related with times, the mean execution time (M) and the standard deviation (SD) taken by the controller in each of the tests were computed. The controller does not take more than $M = 11.5\ ms$ on average with a maximum standard deviation of $SD = 3.9$. With this, it is proposed that the implementation can be tested with the real-time system, without any significant delays generated by the calculation of the control action.

4 DISCUSSION

As an analysis of the tests presented in section 2.1, which involved eleven trials, the model of the rehabilitation system has an appropriate behavior, therefore it was validated. In the tests described in section 2.2, the results with the six exercises show that the system may follow several desired trajectories. The ISE compared with the references entered in the system are small, and may be despised. Therefore, it is considered that the controller is capable of manipulating the torque of the joints, so that it follows specific trajectories. According to that, the controller is able to manipulate the three torques at the same time, hence it is possible to follow specific trajectories. Taking into account the mean execution time (M) and the standard deviation (SD) taken by the controller within the BBB, it is proposed that this system can be tested in real-time, without notable delays related with the movement control algorithm.

5 CONCLUSION AND FUTURE WORK

The tests of the model showed that when the CTC algorithm is deactivated, a three-segment pendulum behavior is obtained, as expected in an RRR robot with no torque in the motors.

Additionaly, we observed that only with the gravitational compensation component of the CTC algorithm, the controller is able to keep the robot in a static position reference, *i.e.*, the initial position.

These simulations have shown the feasiblility of implementing a HIL simulation in order to control the movements of a simplified model of Nukawa. How-

Table 5: Model validation trials.

Trial	Tu	Initial Position (°, °, °)	Backrest Position (°)	Reference	ISE Normalized	Description
A1	Tu	(0,0,90)	180	Hold	(5.0e-07, 1.5e-06, 2.5e-08)	No movement was observed, the motors were not saturated. The ISE error may be despised
A2	Tu	(-90,0,90)	90	Hold	(3.1e-08, 2.0e-09, 3.8e-08)	No movement was observed, the motors were not saturated. The ISE error may be despised
A3	Tu	(0,-90,90)	90	Hold	(1.5e-07, 1.4e-08, 5.7e-08)	No movement was observed, the motors were not saturated. The ISE error may be despised
B1	0	(0,0,90)	180	Hold	(8.683e+03, 361.3, 2.809e+03)	The robot fell as a pendulum with a big oscillation of the hip joint, the motors did not perform any torque. The ISE error shows that the system failed to hold the position
B2	0	(-90,0,90)	90	Hold	(7.3, 103.4, 2.004e+03)	The robot dropped as a pendulum with a small oscillation of the hip joint, the motors did not perform any torque. The ISE error shows that the system failed to hold the position with a big movement of the ankle joint
B3	0	(0,-90,90)	90	Hold	(7.206e+03, 5.162e+03, 3.577e+03)	The robot dropped as a pendulum with a big oscillation of the hip, knee and ankle joint, the motors did not perform any torque. The ISE error shows that the system failed to hold the position
C1	Gc	(0, 0, 90)	90	Hold	(2.0e-04, 1.4e-05, 4.5e-08)	The robot stayed at the initial position, and no saturation occurred. The ISE error may be despised
C2	Gc	(-90,0,90)	90	Hold	(4.3e-08, 1.3e-17, 4.3e-08)	The robot stayed at the initial position, and no saturation occurred. The ISE error may be despised
C3	Gc	(-90,0,90)	90	Hold	(3.0e-04, 2.8e-08, 4.9e-08)	The robot stayed at the initial position, and no saturation occurred. The ISE error may be despised
D	Vc	(0,0,90)	90	Hold	(7.7e+03, 454.1, 1.488e+03)	The robot dropped as a pendulum with a big oscillation of the hip, knee and ankle joint, the motors did not perform any torque. The ISE error shows that the system failed to hold the position
E	Mc	(0,0,90)	90	Hold	(8.464e+03, 454.154, 1.488e+03)	The robot dropped as a pendulum with a big oscillation of the hip, knee and ankle joint. The ISE error shows that the system failed to hold the position

ever, the computational model may differ from the physical, due to the fact of simplifications or inaccuracies. Therefore, a future work requires to conduct these tests with the actual robotic system.

The use of the development platform Beablebone Black Rev C (BBB) proved to be useful for the implementation of the CTC control since the response time is in an acceptable range, *i.e.*, it is lower than the sampling period. In addition, the performance of the control algorithm implemented in Beagle Bone Black Rev C (BBB) may be evaluated in other development platforms such as the new Raspberry Pi 3, and others.

The Hardware-In-The-Loop (HIL) simulation of the mathematical model with the dynamics of the Nukawa rehabilitation system allowed to validate the CTC control algorithm without the need to have the actual robot and thus to make variations in the control parameters and to evaluate the system response.

In order to obtain a model closer to the real one, before testing the controller, it is imperative to configure the system with known lengths and weights, and to drop it from the Position $q = (0\,^\circ,\ 0\,^\circ,\ 90\,^\circ)$, without restrictions or mechanical limits enabled. During this test the position of each joint must be acquired and then, an optimization algorithm must be used in order to tune the friction coefficients. Preliminary tests, show that the value of the dynamic friction influences in the behavior of the system, *e.g.*, when the constant $kfr = 0$, the system behaves like a system without friction and stays oscillating without losing

Table 6: Results of the six HIL simulations using predefined trajectories extracted from ACL rehabilitation exercises executed by a physiotherapist and acquired with three twin-axis goniometers.

Exercise	Backrest Angle (°)	ISE Normalized	Maximum Torque (Nm, Nm, Nm)	Minimum Torque (Nm, Nm, Nm)	Maximum Angle (°, °, °)	Minimum Angle (°, °, °)
1	180	(19.6, 8.5, 5.2)	(727.6, 278.6, 64.4)	(-113.8, -85.1, -51.5)	(50.1, -0.3, 68.7)	(2.8, -15.6, 59.4)
2	180	(41.6, 92.3, 7.9)	(424.7, 181.0, 19.9)	(-131.9, -1.1, -37.0)	(101.0, -8.8, 81.0)	(38.0, -57.2, 65.1)
3	90	(2.7, 30.3, 31.4)	(491.4, 207.1, 71.8)	(211.4, 20.6, -10.0)	(5.0, -17.9, 78.3)	(-5.1, -70.7, 52.7)
4	90	(2.2, 25.8, 42.1)	(453.3, 170.2, 74.6)	(212.3, 55.9, -34.1)	(4.1, -29.9, 130.0)	(-4.4, -63.8, 82.7)
5	90	(2.3, 24.2, 33.1)	(433.5, 142.1, 69.8)	(259.7, 62.9, -40.3)	(13.9, -29.9, 130.0)	(6.2, -62.6, 82.7)
6	165	(5.7, 37.4, 21.2)	(477.2, 176.4, 75.4)	(153.1, 15.2, 2.4)	(46.5, -57.7, 83.3)	(24.9, -101.8, 69.6)

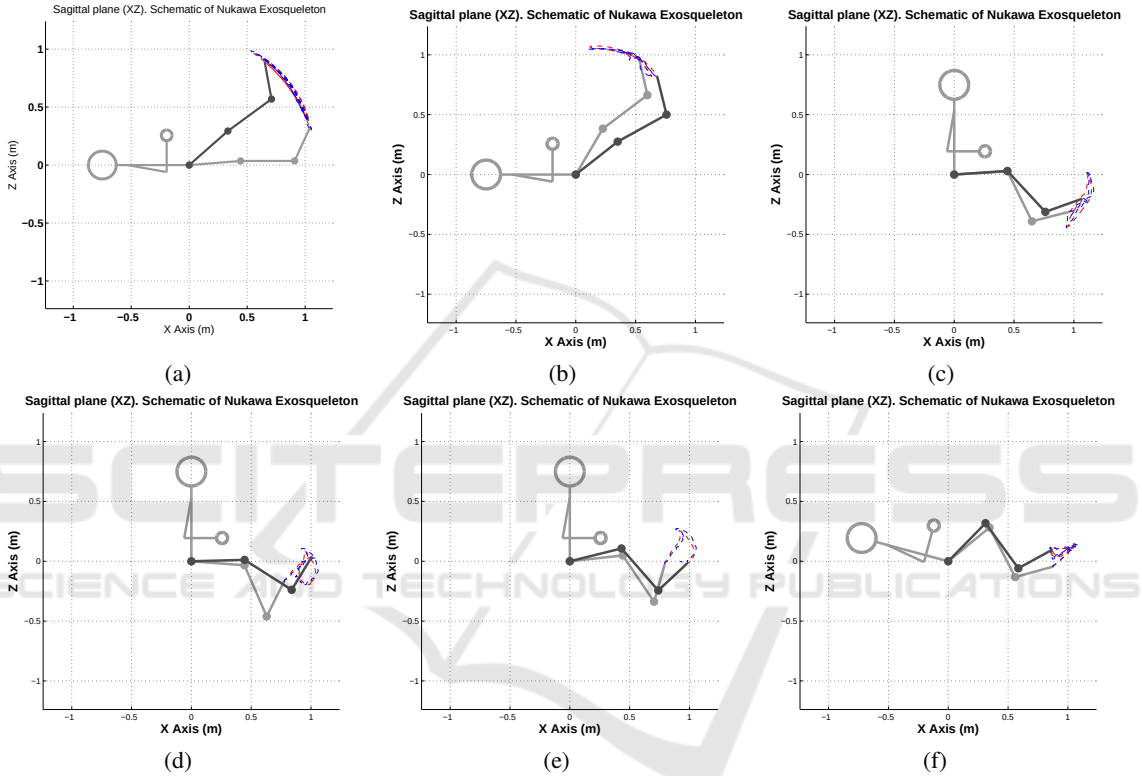

Figure 5: HIL Simulation of the Nukawa using a trajectory extracted during the six exercises.

energy. On the other hand, when kfr increases the system oscillates fewer times.

It is considered as future work the inclusion of the static friction in the mathematical model of the robot, which would allow to take into account the force that is opposed to the beginning of the movement, *i.e.*, including the static friction would include the effects that may generate a dead zone for the controller. Even though a slightly larger torque is exerted, no movement will be generated until it is able to overcome static friction. In addition, it is possible to include the friction that occurs between the robot and the patient with the air.

Some of the perturbations of the system may be known a priori, therefore, it is proposed that in the future they may be included in the CTC algorithm, in order to make a feedforward control, *e.g.*, using an estimate of the dynamic and static friction in the algorithm of CTC, in order to compensate the perturbations that the system can suffer due to these and thus, not leave all the work to the external loop controller, facilitating the work.

Another future work is to use the 3D model of Nukawa or even to do experimental tests with the actual robot, to calculate the center of mass of each limb, as well as to use the models proposed by De Leva, in order to obtain a mathematical model closer to the real one.

In the future, HIL simulation tests can be performed using speed, acceleration or force references rather than position references. These test may be conducted in order to control the torque of the motors

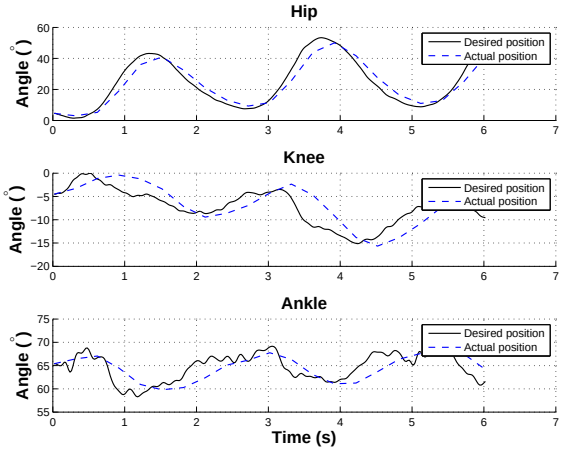

Figure 6: Desired position vs actual position of each joint of the Nukawa during a HIL Simulation using a trajectory extracted during an elevation of straight leg exercise.

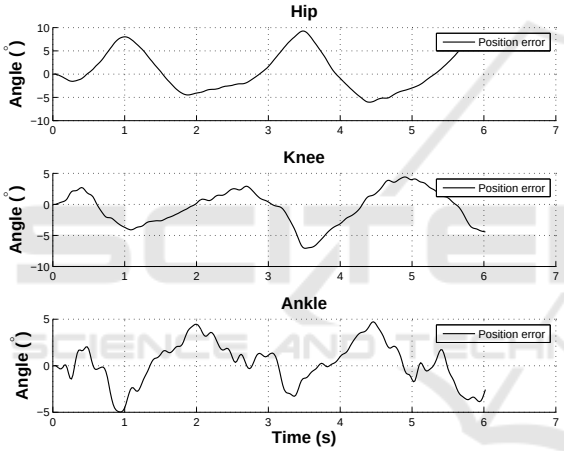

Figure 7: Position error of each joint of the Nukawa during a HIL Simulation using a trajectory extracted during an elevation of straight leg exercise.

to perform other type of exercises rather than isokinetic, *e.g.*, Isotonic.

Further work, also includes implementing the control algorithm in the Robot Operating System (ROS), and implementing the simulations in an environment other than Matlab such as Gazebo, V-REP, Peekabot, Webots, Drake, among others.

Finally, the system was able to reproduce the trajectories associated with the phases 2 and 4 considering The Accelerated Reconstruction Rehabilitation Program of Chester, phase 1 and 2 of the Classic 1981 Protocol and pre-operatory and post-operatory phase in Steadman Protocol of Anterior Cruciate Ligament (ACL) rehabilitation protocols. This will allow to validate in the future different types of exercises that include these trajectories, *i.e.*, isotonic, assisted, resisted, among others.

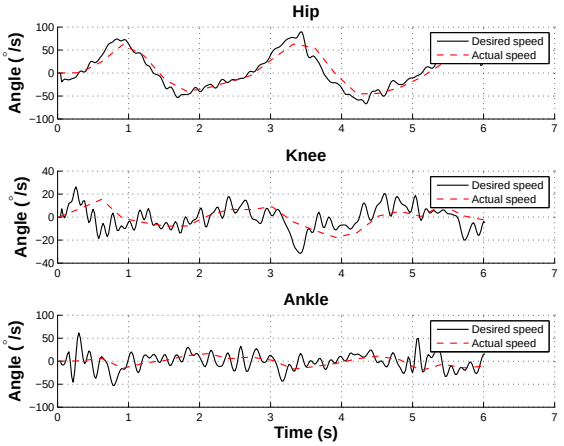

Figure 8: Desired speed vs actual speed of each joint of the Nukawa during a HIL Simulation using a trajectory extracted during an elevation of straight leg exercise.

The constants of the outer loop were set using an heuristic PD tuning method, these methods and values were appropriate for the current application. However, it could be a better approach if an optimization method is used, *i.e.*, an autotuning method.

Further work, also includes acquiring the same trajectories during the six exercises with a group of subjects, moreover, with patients in order to compare the trajectory execute by both, healthy and unhealthy subjects and to propose trajectories that fit all subjects.

ACKNOWLEDGEMENTS

The authors would like to express their sense of gratitude to the engineer Juan G. Patiño and the magister Florian Kirby for their help modelling the robotic system, and conducting the offline simulations. We thank “IPS ARTHROS” and the “Centro de MVMT”, for providing the facilities for the tests. We also thank the physiotherapy student Lina loaiza, and intern in “IPS ARTHROS” for her help with the execution of the tests. We thank the electronic engineer Mario Portela and the mechanical engineer Juan Guillermo Madrid, for their support during the acquisition of technical information of the robotic system Nukawa. Finally, we sincerely thank the “Departamento Administrativo de Ciencia, Tecnología e Innovación (Colciencias)” for their grant within the project called “MyoLegSys” with agreement 836-2015.

REFERENCES

Akdogan, E. and Adli, M. A. (2011). The design and control of a therapeutic exercise robot for lower limb rehabilitation: Physiotherabot. *Mechatronics*, 21(3):509–522.

American Academy of Orthopaedic Surgeons (2011). *Sports Medicine Media Guide an Illustrated Resource on the Most Common Injuries and Treatments in Sports*.

Arosha Senanayake, S. M. N., Malik, O. A., Iskandar, P. M., and Zaheer, D. (2014). A knowledge-based intelligent framework for anterior cruciate ligament rehabilitation monitoring. *Applied Soft Computing Journal*, 20:127–141.

Augusta, V. (2013). Comparación entre diferentes procedimientos de ajuste de controladores PID. I. Valores máximos de la variable controlada y de la señal reguladora.

Biometrics Ltd (1998). Goniometer and torsiometer operating manual. Technical report.

Blaya, J. a. and Herr, H. (2004). Adaptive Control of a Variable-Impedance Ankle-Foot Orthosis to Assist Drop-Foot Gait. *IEEE Transactions on Neural Systems and Rehabilitation Engineering*, 12(1):24–31.

Cimino, F., Volk, B. S., and Setter, D. (2010). Anterior cruciate ligament injury: Diagnosis, management, and prevention. *American Family Physician*, 82(8):917–922.

De Leva, P. (1996). Adjustments to zatsiorsky-seluyanov's segment inertia parameters. *Journal of Biomechanics*, 29(9):1223–1230.

Departamento Administrativo Nacional de Estadísctica (2004). Información estadística de la discapacidad.

Dollar, A. M. and Herr, H. (2008). Lower extremity exoskeletons and active orthoses: Challenges and state-of-the-art. *IEEE Transactions on Robotics*, 24(1):144–158.

Eby, W. R. (2005). Feasibility Analysis of a Powered Lower-Limb Orthotic for the Mobility Impaired User by. *Simulation*.

Eurostat (2014). Disability statistics - prevalence and demographics. 2011(September):1–5.

Ganley, T. J. (2011). Preface: ACL Injuries in the Young Athlete: A Focus on Prevention and Treatment. *Clinics in Sports Medicine*, 30(4):xv–xviii.

Guizzo, E. and Goldstein, H. (2005). The rise of the body bots [robotic exoskeletons. *IEEE Spectrum*, 42(10):50–56.

K. S. Fu, R.C. Gonzalez, C. L. (1987). *Robotics: Control, Sensing, Vision, and Intelligence*. Mcgraw-Hill Book Company.

Kiguchi, K., Tanaka, T., and Fukuda, T. (2004). Neuro-fuzzy control of a robotic exoskeleton with EMG signals. *IEEE Transactions on Fuzzy Systems*, 12(4):481–490.

Kirby, F. (2016). Simulación de los algoritmos de control de un sistema de rehabilitación de miembro inferior (LegSys). Master's thesis, Universidad Pontificia Bolivariana.

Lasso, I. L., Masso, M., and Vivas, O. A. (2010). Exoesqueleto para reeducación muscular en pacientes con IMOC tipo diplejía espástica moderada. pages 1 – 88.

Li, A. Y. and Ng, G. Y. (2004). Overview of Anterior Cruciate Ligament Rehabilitation and its Evolution in Hong Kong in the Past 8 Years. *Hong Kong Physiotherapy Journal*, 22(1):14–21.

Machhindra, V., Lal, H., Chowdhury, B., Dev, C., Meena, S., and Kumar, K. (2016). ScienceDirect Arthroscopic anatomic double bundle anterior cruciate ligament reconstruction : Our experience with follow-up of 4 years. 7:3–8.

Nancy Berryman, W. D. B. P. (2002). *Joint Range of Motion and Muscle Length Testing*. 1st edition.

Nguyen-Tuong, D. and Peters, J. (2008). Learning robot dynamics for computed torque control using local Gaussian processes regression. *Proceedings of the 2008 ECSIS Symposium on Learning and Adaptive Behaviors for Robotic Systems, LAB-RS 2008*, pages 59–64.

Olaya, A. R. (2008). Sistema robótico multimodal para análisis y estudios en biomecánica, movimiento humano y control neuromotor. pages 1–256.

Pan, D., Gao, F., Miao, Y., and Cao, R. (2015). Co-simulation research of a novel exoskeleton-human robot system on humanoid gaits with fuzzy-PID/PID algorithms. *Advances in Engineering Software*, 79:36–46.

Patiño, J. G., Bravo, E. E., Perez, J. J., and Perez, V. (2013). Lower limb rehabilitation system controlled by robotics, electromyography surface and functional electrical stimulation. *Pan American Health Care Exchanges, PAHCE*, (2002):6257.

Piriyaprasarth, P., Morris, M. E., Winter, A., and Bialocerkowski, A. E. (2008). The reliability of knee joint position testing using electrogoniometry. *BMC musculoskeletal disorders*, 9:6.

Plagenhoef, S., Evans, F. G., and Abdelnour, T. (1983). Anatomical Data for Analyzing Human Motion. *Research Quarterly for Exercise and Sport*, 54(2):169–178.

Pratt, J., Krupp, B., Morse, C., and Collins, S. (2004). The RoboKnee: an exoskeleton for enhancing strength and endurance during walking. *IEEE International Conference on Robotics and Automation, 2004. Proceedings. ICRA '04. 2004*, 3(April):2430–2435.

World Health Organization (2011). World Report on Disability. Technical report, World Health Organization, Ginebra.

Yan, T., Cempini, M., Oddo, C. M., and Vitiello, N. (2015). Review of assistive strategies in powered lower-limb orthoses and exoskeletons. *Robotics and Autonomous Systems*, 64:120–136.

Zoss, A. B., Kazerooni, H., and Chu, A. (2006). Biomechanical Design of the Berkeley Lower Extremity Exoskeletong (BLEEX). *IEEE/ASME Transactions on Mechatronics*, 11(2):128–138.